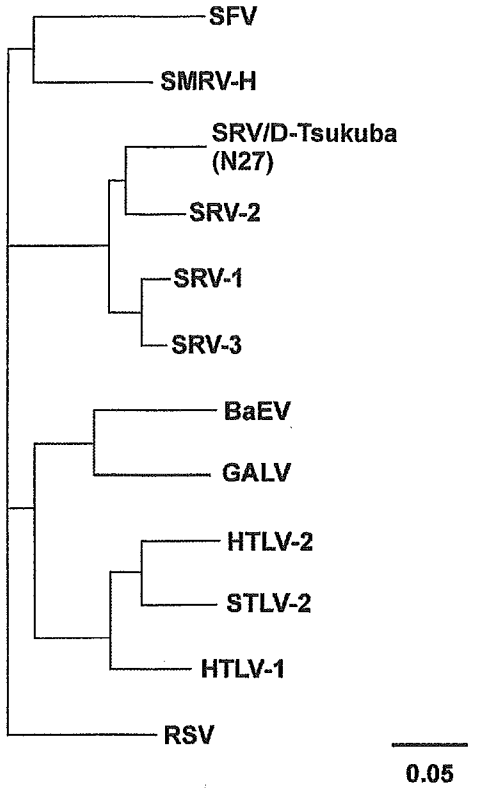

Fig. 3. Phylogenic analysis of SRV/D-T (N27 strain) gag sequence and other retrovirus *gag* genes. The phylogenetic tree was constructed by the NJ method based on the entire 1980-bp *gag* gene of the SRV/D N27 isolates. Branch lengths are proportional to estimated number of substitutions per site, which represent the evolutional distance.

SRV/D-2 serum in an indirect fluorescent assay; and (4) electron microscopic analysis of infected cells clearly demonstrated the presence of virions having a type D morphology (Figs. 1C,D). Therefore, we have designated the two SRV/D isolates from cynomolgus monkeys SRV/D-T.

The entire *gag* gene nucleotide sequence and deduced amino acid sequence of the N27 isolate had high homology to other known SRVs (Fig. 2, Table 1), and this close similarity extended to individual post-translational proteolytic products (p10, p12, p27, p14 and p4; Fig. 2) [26,27]. The highest homology was observed in the p10 and p27 regions, while the homology in p12 and p14 was somewhat lower (Table 2). Also, phylogenetic analyses confirmed that the N27 strain is closely related to, but distinct from, the other three known SRV/Ds (Fig. 3).

In relation to SRV/D-5, we compared the *gag* sequence of our N27 isolate (629 bp) with the published *gag-prt* region of SRV/D-5 [9]. Homology was 84.1%, whereas homology between the N27 and T150 isolates was 99.7%. Furthermore, the homology between the N27 and T150 isolates and SRV/D-1, -2 and -3 was in a range of 82.8–83.5. Accordingly, the N27 and T150 isolates are essentially the same and closely related to, but distinct from, SRV/D-1, -2, -3 and -5. Regarding SRV-6, the Indian Hanuman langur from which this virus was isolated belongs to a completely different genus and its resident area is different from that of the TPC cynomolgus monkeys imported 25 years ago [30]. Therefore, even though sequences are not available for direct comparison, we do not think our SRV/D isolates are likely to be identical to SRV-6.

The relationship of the N27 and T150 isolates to SRV/D-4 is less clear. SRV/D-4 is known only from a single isolate obtained from a cynomolgus monkey in California [13]. Only when sequence data become available for this isolate will we be able to confirm this. Although we detected 461- and 400-bp PCR products using published primer sets [14] which detect the p27 region of SRV/D-1 to -5, a 232-bp band was also detected upon nested PCR with primers that amplify SRV/D-1, -2 and -3 [13] but do not amplify SRV/D-4 and -5 (N.W. Lerche, California National Primate Research Center, USA, personal communication). Thus, we do not believe that our SRV/D isolate is the same as SRV/D-4 or -5.

Reconciling the results of the PCR detection and morphological study, the N27 and T150 isolates appear to be more closely related to SRV/D-2 and SRV/D-1 and -3 than to SRV/D-4 or -5. Therefore, we have tentatively designated the N27 and T150 isolates as strain SRV/D-T. Complete genome sequence analysis and comparison of all the SRV/D subtypes will be necessary to definitively classify these viruses.

Acknowledgements

We thank to Dr. Fumiko Ono and Dr. Naohide Ageyama and the animal caretakers at The Corporation for Production and Research of Laboratory Primates for giving us daily information of the monkey health conditions. We also thank Dr. R. Eberle (Department of Veterinary Pathobiology, Oklahoma State University College of Veterinary Medicine) for critical reading of the manuscript. We thank Shionogi and Co., Ltd. for providing recombinant IL-2. This work was supported in part by a grant from the ministry of Health, Labor, and Welfare of Japan.

References

[1] R.V. Henrickson, D.H. Maul, K.G. Osborn, J.L. Sever, D.L. Madden, L.R. Ellingsworth, et al., Epidemic of acquired immunodeficiency in rhesus monkeys, Lancet 1 (1983) 388–390.

[2] M.B. Gardner, P. Luciw, N. Lerche, P. Marx, Nonhuman primate retrovirus isolates and AIDS, Adv. Vet. Sci. Comp. Med. 32 (1988) 171–226.

[3] P.A. Marx, D.H. Maul, K.G. Osborn, N.W. Lerche, P. Moody, L.J. Lowenstine, et al., Simian AIDS: isolation of a type D retrovirus and transmission of the disease, Science 223 (1984) 1083–1086.

[4] M.D. Daniel, N.W. King, N.L. Letvin, R.D. Hunt, P.K. Sehgal, R.C. Desrosiers, A new type D retrovirus isolated from macaques with an immunodeficiency syndrome, Science 223 (1984) 602–605.

[5] K. Stromberg, R.E. Benveniste, L.O. Arthur, H. Rabin, W.E. Giddens Jr., H.D. Ochs, et al., Characterization of exogenous type D retrovirus from a fibroma of a macaque with simian AIDS and fibromatosis, Science 224 (1984) 282–289.

[6] M.D. Power, P.A. Marx, M.L. Bryant, M.B. Gardner, P.J. Barr, P.A. Luciw, Nucleotide sequence of SRV-1, a type D simian acquired immune deficiency syndrome retrovirus, Science 231 (1986) 1567–1572.

[7] P. Sonigo, C. Barker, E. Hunter, S. Wain-Hobson, Nucleotide sequence of Mason–Pfizer monkey virus: an immunosuppressive D-type retrovirus, Cell 45 (1986) 375–385.

[8] R.M. Thayer, M.D. Power, M.L. Bryant, M.B. Gardner, P.J. Barr, P.A. Luciw, Sequence relationships of type D retroviruses which cause simian acquired immunodeficiency syndrome, Virology 157 (1987) 317–329.

[9] B. Li, M.K. Axthelm, C.A. Machida, Simian retrovirus serogroup 5: partial *gag-prt* sequence and viral RNA distribution in an infected rhesus macaque, Virus Genes 21 (2000) 241–248.

[10] J.S. Nandi, V. Bhavalkar-Potdar, S. Tikute, C.G. Raut, A novel type D simian retrovirus naturally infecting the Indian Hanuman langur (*Semnopithecus entellus*), Virology 277 (2000) 6–13.

[11] J.S. Nandi, S.A. Tikute, A.K. Chhangani, V.A. Potdar, M. Tiwari-Mishra, R.A. Ashtekar, J. Kumari, A. Walimbe, S.M. Mohnot, Natural infection by simian retrovirus-6 (SRV-6) in Hanuman langurs (*Semnopithecus entellus*) from two different geographical regions of India, Virology 311 (2003) 192–201.

[12] C.C. Tsai, W.E. Giddens Jr., H.D. Ochs, W.R. Morton, G.H. Knitter, G.A. Blakley, et al., Retroperitoneal fibromatosis and acquired immunodeficiency syndrome in macaques: clinical and immunologic studies, Lab. Anim. Sci. 36 (1986) 119–125.

[13] N.W. Lerche, R.F. Cotterman, M.D. Dobson, J.L. Yee, A.N. Rosenthal, W.M. Heneine, Screening for simian type-D retrovirus infection in macaques, using nested polymerase chain reaction, Lab. Anim. Sci. 47 (1997) 263–268.

[14] N.W. Lerche, W.M. Switzer, J.L. Yee, V. Shanmugam, A.N. Rosenthal, L.E. Chapman, T.M. Folks, W. Heneine, Evidence of infection with simian type D retrovirus in persons occupationally exposed to nonhuman primates, J. Virol. 75 (2001) 1783–1789.

[15] M. Kimura, A simple method for estimating evolutionary rates of base substitutions through comparative studies of nucleotide sequences, J. Mol. Evol. 16 (1980) 111–120.

[16] N. Saitou, M. Nei, The neighbor-joining method: a new method for reconstructing phylogenetic trees, Mol. Biol. Evol. 4 (1987) 406–425.

[17] G.H. Marracci, R.D. Kelley, K.Y. Pilcher, L. Crabtree, S.M. Shiigi, N. Avery, et al., Simian AIDS type D serogroup 2 retrovirus: isolation of an infectious molecular clone and sequence analyses of its envelope glycoprotein gene and 3′ long terminal repeat, J. Virol. 69 (1995) 2621–2628.

[18] S. Kato, K. Matsuo, N. Nishimura, N. Takahashi, T. Takano, The entire nucleotide sequence of baboon endogenous virus DNA: a chimeric genome structure of murine type C and type D retroviruses, Jpn. J. Genet. 62 (1987) 127–137.

[19] T. Oda, S. Ikeda, S. Watanabe, M. Hatsushika, K. Akiyama, F. Mitsunobu, Molecular cloning, complete nucleotide sequence, and gene structure of the provirus genome of a retrovirus produced in a human lymphoblastoid cell line, Virology 167 (1988) 468–476.

[20] S. Delassus, P. Sonigo, S. Wain-Hobson, Genetic organization of gibbon ape leukemia virus, Virology 173 (1989) 205–213.

[21] J.J. Kupiec, A. Kay, M. Hayat, R. Ravier, J. Peries, F. Galibert, Sequence analysis of the simian foamy virus type 1 genome, Gene 101 (1991) 185–194.

[22] T.M. Zhao, M.A. Robinson, S. Sawasdikosol, R.M. Simpson, T.J. Kindt, Variation in HTLV-I sequences from rabbit cell lines with diverse in vivo effects, Virology 195 (1993) 271–274.

[23] K. Shimotohno, D.W. Golde, M. Miwa, T. Sugimura, I.S. Chen, Nucleotide sequence analysis of the long terminal repeat of human T-cell leukemia virus type II, Proc. Natl. Acad. Sci. USA 81 (1984) 1079–1083.

[24] M. Van Brussel, M. Salemi, H.F. Liu, J. Gabriels, P. Goubau, J. Desmyter, et al., The simian T-lymphotropic virus STLV-PP1664 from *Pan paniscus* is distinctly related to HTLV-2 but differs in genomic organization, Virology 243 (1998) 366–379.

[25] W.A. Haseltine, A.M. Maxam, W. Gilbert, Rous sarcoma virus genome is terminally redundant: the 5′ sequence, Proc. Natl. Acad. Sci. USA 74 (1977) 989–993.

[26] J. Bradac, E. Hunter, Polypeptides of Mason–Pfizer monkey virus. I. Synthesis and processing of the gag-gene products, Virology 138 (1984) 260–275.

[27] L.E. Henderson, R. Sowder, G. Smythers, R.E. Benveniste, S. Oroszlan, Purification and N-terminal amino acid sequence comparisons of structural proteins from retrovirus-D/Washington and Mason–Pfizer monkey virus, J. Virol. 55 (1985) 778–787.

[28] R.E. Guzman, R.L. Kerlin, T.E. Zimmerman, Histologic lesions in cynomolgus monkeys (*Macaca fascicularis*) naturally infected with simian retrovirus type D: comparison of seropositive, virus-positive, and uninfected animals, Toxicol. Pathol. 27 (6) (1999) 672–677.

[29] L.L. Rosenblum, R.A. Weiss, M.O. McClure, Virus load and sequence variation in simian retrovirus type 2 infection, J. Virol. 74 (8) (2000) 3449–3454.

[30] S. Honjo, The Japanese Tsukuba Primate Center for Medical Science (TPC): an outline, J. Med. Primatol. 14 (1985) 75–89.

NEW E-submission site

The recently launched e-submission website enables authors to electronically submit their articles to the journal ***Microbes and Infection.*** Electronic submission offers numerous advantages over the traditional procedure of sending your manuscript by regular mail:

- you will be immediately informed that your paper has been received
- the processing time to publication will be greatly reduced by the use of an internet-based workflow
- your article, once accepted, will be displayed freely online right up until it is compiled in the printed issue and then becomes available online through ScienceDirect (http://www.sciencedirect.com)

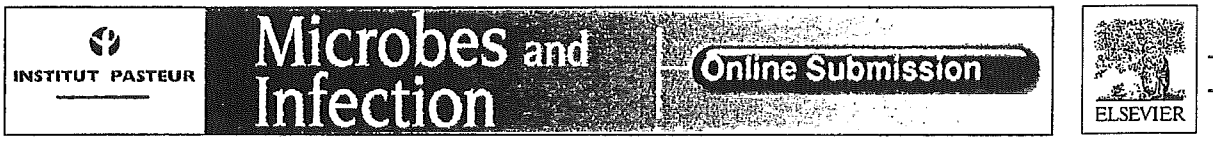

Some frequently asked questions:

Do I need to create a PDF document?

No. Your file will be converted by us to PDF.

What kind of files should I submit?

For the text, MS Word and WordPerfect files are accepted.
As graphics files you may submit TIFF, EPS or JPEG.

What should I prepare ahead of time for the submission?

- the complete article as an MS Word or WordPerfect file with all graphics embedded, prepared according to instructions in the guidelines and in the instructions for manuscript preparation
- all figures as separate valid graphics files
- the choice of your Editor
- the first names, last names, e-mail addresses and affiliations of the main author and all co-authors
- the manuscript title
- the manuscript keywords

What happens after I have successfully completed submission?

You will receive acknowledgement of receipt of your article by the Editor, who will provide you with an identification number. Your manuscript will then be examined by the Editor and forwarded to selected referees. An e-mail message from the Editor will notify you about its status: acceptance, rejection or need for revision. After acceptance of the manuscript, it will be checked for linguistic correctness by the journal's editorial manager and published online thereafter.

For submission guidelines and to submit your paper online visit:

http://pasteur.fontismedia.com/mic/

Comparative Medicine
Copyright 2005
by the American Association for Laboratory Animal Science

Vol 55, No 2
April 2005
Pages 145-149

Survey of Captive Cynomolgus Macaque Colonies for SRV/D Infection Using Polymerase Chain Reaction Assays

Masayuki Hara,[1,2] Toshihiko Kikuchi,[1] Fumiko Ono, DVM, PhD,[3] Jun-ichirou Takano,[3] Naohide Ageyama, DVM,[3] Koji Fujimoto,[3] Keiji Terao, PhD,[1] Tadashi Baba, PhD,[2] and Ryozaburo Mukai, PhD[1,*]

The exogenous simian type D retroviruses (SRV/Ds) are prevalent in macaque monkeys and sometimes cause immunodeficiency with anemia, weight loss, and persistent unresponsive diarrhea. SRV/D isolates are classified as subtypes 1 to 6, and the entire sequences of the *gag* region of SRV/D-1, -2, and -3 and SRV/D-Tsukuba (SRV/D-T) have been determined. We designed specific primers in the *gag* region of SRV/D-T that enabled us to directly detect by polymerase chain reaction (PCR) SRV/D-T proviral DNA sequences in DNA extracted from whole blood. Using this assay and another PCR assay that detects multiple SRV/D subtypes, we performed a survey for SRV/D infection in our specific pathogen-free (SPF) and conventional colonies at Tsukuba Primate Center (TPC). In the SPF colony, no SRV/D signal was detected in any animal. On the other hand, SRV/D-T was detected in 11 of 49 animals (22.5%) in the conventional colony. SRV/D-T was the only SRV/D subtype detected. Consequently, SRV/D-T is the major SRV/D subtype present in cynomolgus monkeys at TPC.

The exogenous simian type D retroviruses (SRV/Ds) are prevalent in colony-born macaques and sometimes cause immunodeficiency with anemia, weight loss, and persistent unresponsive diarrhea (2, 3, 5, 12). Macaques are needed for a variety of biomedical studies such as preclinical studies in regenerative medicine, safety testing for vectors in gene therapy, and developing AIDS vaccines using simian immunodeficiency virus (SIV or SHIV) (1, 9, 13).

If macaques infected with SRV/D are used in such experiments, the results may be affected by the animal's condition due to the onset of clinical signs of SRV/D induced diseases including immunodeficiency, and in the worst case, increased mortality may result in the loss of research monkeys (9). Therefore, the eradication of SRV/D from macaque breeding colonies is of great importance. Unlike other viral agents (e.g., herpesviruses and measles virus), some monkeys may carry SRV/D without having detectable serum antibodies. Therefore, it is necessary to perform both serologic testing and detection of viral presence. Because virus isolation is time- and labor-intensive, detection of SRV/D proviral DNA using polymerase chain reaction (PCR) technology has been used as a rapid and effective testing method. In addition, PCR tests that simultaneously detect multiple SRV/D serotypes have been reported (8, 23).

SRV/Ds are classified into subtypes 1 to 6, and the entire genome sequences of SRV/D-1, -2, and -3 have been determined (17, 19, 21). Recently, part of the *gag-prt* sequence of SRV-5 was determined (11), and SRV/D-6 has been isolated from a Hanuman langur (*Semnopithecus entellus*) (15). We recently described the isolation of SRV/D-T from cynomolgus monkeys in the breeding colony at the National Institute of Infectious Diseases (NIID; Tokyo, Japan) and reported the sequence of the *gag* region of this isolate (4). The SRV/D-T subtype was isolated from two cynomolgus monkeys in the conventional breeding colony at TPC. However, it is not known whether this subtype was isolated by chance or if it is prevalent in the colony. In order to survey the SRV/D subtypes prevalent in our breeding colony, we designed an SRV/D-T-specific PCR primer set based on the sequences of the *gag* regions of SRV/D -1, -2, and -3 and SRV/D-T. To increase the sensitivity of PCR detection, an SRV/D-T-specific nested primer set also was designed. Here, we report the extent of infection with SRV/D in cynomolgus monkeys from our specific pathogen-free (SPF) and conventional colonies by using a direct PCR detection method with ethlylenediamine tetraacetic acid (EDTA)-treated whole blood and the SRV/D-T-specific primer set and other published primer sets that detect multiple SRV/Ds.

Materials and Methods

Humane care and use of animals. All procedures involving the use of animals in this study conformed to the Rules for Animal Care and Management of Tsukuba Primate Center (6) and the Guiding Principles for Animal Experiments Using Nonhuman Primates formulated by the Primate Society of Japan (18). Housing and care procedures were approved by the Animal Welfare and Animal Care Committee of the National Institute of Infectious Diseases (Tokyo, Japan).

Colony description. For initial establishment of the indoor cynomolgus monkey breeding colony at TPC, monkeys (*Macaca fascicularis*) were imported from the Philippines, Indonesia, and Malaysia from 1979 to 1983. Since this time, most monkeys have

Received: 8/22/04. Revision requested: 10/4/04. Accepted: 12/7/04.
[1]Tsukuba Primate Center for Medical Science National Institute Infectious Diseases (NIID), 1 Hachimandai, Tsukuba, 305-0843 Japan; [2]Graduate School of Life and Environmental Sciences, and Institute of Applied Biochemistry, University of Tsukuba, 1-1-1 Tennodai, Tsukuba 305-8572, Japan; [3]The Corporation for Production and Research of Laboratory Primates, 1 Hachimandai, Tsukuba, 305-0843 Japan.
[*]Corresponding author.

Table 1. Polymerase chain reaction (PCR) primer sets for detection of simian type D retroviruses (SRV/D)

Name	Sequence (5' to 3')	Product size (bp)	Subtype detected	Region
Tga1[a]	GGGCTAAAGCCTCGACAA	722	SRV/D-T	gag
Tga2	AGACTTCCACAGTAGGTGAT			
Tga3[a]	GAAGAAAAAGGTACCCAATGA	381	SRV/D-T	gag
Tga4	GGCACAGGAGAAGAGTCTTT			
SRVPOLF1[b]	TACCAITICCTCATTTIGGAGTTAATCC	446	SRV/D-1 to –5	pol
SRVPOLR1	AAAGAGTGCITGATTGAGIATITTCCTG			
SRVPOLF2[b]	RITICCCAAIAATGITITGGCAAATGGA	181	SRV/D-1 to –5	pol
SRVPOLR2	AGGIIGICCAAATAATAGAGAAGCAATG			
WH1[c]	CCGCTGTGATGGCGGTAGTCAATCC	268	SRV/D-2	gag
WH3	CTGGGAAAATATCCTTGGGAGGATATTC			
RC14[c]	CAATCCTAAAGAGGAACTCAAAGA	222	SRV/D-2	gag
RC15	TATTCTTCTGTGTTTTTATTAATAAGG			
WH1[c]	CCACTGTAATGGCGGTTGTTAATCC	268	SRV/D-1 and –3	gag
WH3	CTGGGAAAATATCTTTTGGGATTTGTTC			
RC12[c]	TAATCCAAAAGAGGAGCTCAAAGA	222	SRV/D-1 and –3	gag
RC13	TTGTTCTTCCTTTTCTCGACTGGC			

[a]SRV/D-T-specific primer set.
[b]The generic primer set for amplifying SRV/D-1 through -5 (10).
[c]The primer sets for simultaneous detection of SRV/D-1,-3, and -2 (8).

been kept in individual cages set in high-efficiency particulate air (HEPA)-filtered, negative-pressure chambers maintained at 23 to 27°C and 50 to 70% humidity with 12 air changes/h. For breeding, a timed mating system is used in which female monkeys are placed in the male macaque's cage for at least 3 days, and pregnancy is confirmed by ultrasonography. About 4 months after birth, infants are separated from their mothers and paired with an infant of similar size. This colony supplies approximately 180 monkeys, including juvenile monkeys and retired breeders, for research every year.

The conventional cynomolgus monkey group used in these studies consisted of 49 retired breeders (21 male and 28 female) ranging in age from 15 to 37 years; the average numbers of mating partners of these monkeys were 25.4 female macaques per male and 7 male monkeys per female, with each female having 0 to 10 (average, 2.8) offspring. These retired breeders were chosen as representatives of our conventional breeding colony in this study for two reasons. First, given the close contact of these animals with many others over several years, if a virus is present in the colony, these individuals should have acquired it. Second, the group size was similar to that of the SPF colony.

Microbiological status. Periodic health examinations of all monkeys in the breeding colony includes serum biochemistry and microbiological testing every 2 years. Bacteriological testing for *Shigella*, *Salmonella*, and mycobacteria was performed on arrival from Southeast Asia. Simian varicella virus (SVV) has been eradicated from the conventional breeding colony on the basis of antibody testing (14). Serological screening for B virus uses an enzyme immunoassay from BioReliance (Rockville, Md.), with follow-up surveillance conducted every 2 years using both SA8 and B virus antigens (20). Therefore, monkeys in the conventional breeding colony are free from *Shigella*, *Salmonella*, mycobacteria, B virus, and SVV.

Besides the conventional cynomolgus monkey breeding colony, TPC maintains a small SPF colony that is free of SRV/D in addition to B virus and SVV. For SRV/D screening, antibody testing is done by Western blotting with SRV/D-2 antigen (BioReliance), and virus isolation uses the Raji cell syncytial assay (2). SRV/D-negative monkeys were transferred into an SPF room (HEPA-filtered and positive pressure). Follow-up surveillance by antibody testing and virus isolation was conducted every 4 months for the first year and every 6 months thereafter.

Template DNAs. Genomic DNA from macaque whole blood treated with EDTA was prepared using a NucleoSpin Blood kit (Macherey-Nagel, Duren, Germany). For testing the specificity of primers, genomic DNA from Raji cells infected with SRV/D-T (Tsukuba isolate) was extracted using the NucleoSpin Blood kit. Genomic DNAs from Raji cells infected with SRV/D-1 and SRV/D-2 were kindly supplied by Dr. N.W. Lerche (California National Primate Research Center, Davis, Calif.). Plasmid DNA containing the SRV/D-T *gag* region fragment (2189 bp) (4) was prepared using a QIAprep Spin miniprep Kit (Qiagen, Tokyo, Japan).

PCR. Primers specific for SRV/D-T were designed based on the aligned SRV/D-1, -2, and -3 and SRV/D-T sequences (GenBank accession nos. M11841, AF126467, M12349, and AB181392, respectively; Table 1). Primers used for simultaneous detection of multiple SRV/D subtypes (8, 10) also are listed in Table 1. First-round PCR amplification was performed with 500 ng of genomic DNA, 20 pmol of each primer, 10 mM, Tris-HCl (pH 8.0), 50 mM KCl, 2 mM $MgCl_2$, 0.2 mM dNTPs, and 2.5 units Takara Ex *Taq* polymerase (TaKaRa, Otzu, Japan) in a total volume of 50 µl. The amplification was performed as follows: initial denaturation at 95°C for 5 min; 35 cycles at 94°C for 1 min, 56°C for 1 min, and 72°C for 1 min; and final extension at 72°C for 10 min. These conditions were used for primer evaluation and for mixed PCR testing. Amplified PCR products were visualized by electrophoresis in 1.2% agarose gels stained with 0.5 mg/ml ethidium bromide under ultraviolet transillumination.

Nested PCR was performed with 2 µl of the first round PCR reaction mixture, 20 pmol of each primer, 10 mM Tris-HCl (pH 8.0), 50 mM KCl, 2 mM $MgCl_2$, 0.2 mM dNTPs, and 2.5 units of Ex *Taq* polymerase (TaKaRa) in a total volume of 50 µl. The am-

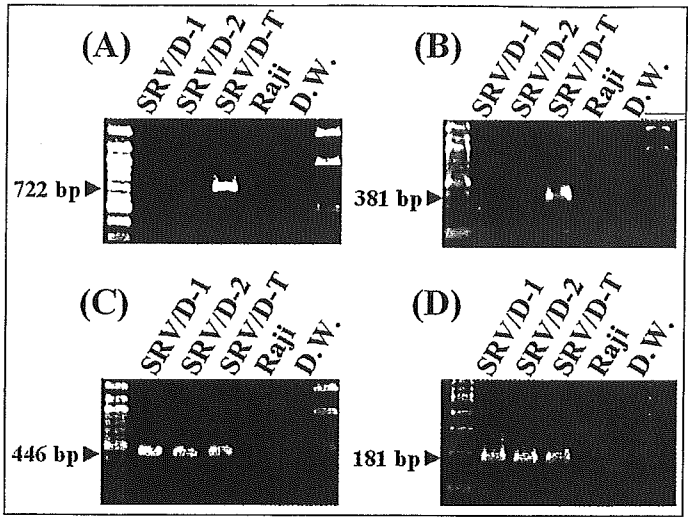

Figure 1. Specific detection of simian type D retrovirus (SRV/D)-T proviral DNA in genomic DNA from Raji cells infected with SRV/D-1, -2, or -T by nested polymerase chain reaction (PCR) assays. (A) Agarose gel electrophoresis of first-round PCR products with the SRV/D-T-specific primers Tga1 and Tga2. (B) Agarose gel electrophoresis of nested PCR products with SRV/D-T-specific primers Tga3 and Tga4. (C) Agarose gel electrophoresis of first-round PCR products with primers SRVPOLF1 and SRVPOLR1for SRV/Ds (10). (D) Agarose gel electrophoresis of nested PCR products with SRV/D-specific primers SRVPOLF2 and SRVPOLR2 (10). DNA size markers, 100-bp ladder (leftmost lane) and 1-kb ladder (far right lane).

plification was performed as follows: initial denaturation at 95°C for 5 min; 30 cycles at 94°C for 1 min, 58°C for 1 min, and 72°C for 1 min; and final extension at 72°C for 10 min.

Sensitivity of SRV/D-T-specific PCR. A 2189 bp gag fragment of SRV/D-T was inserted in pCR2.1 vecter (Invitrogen, Tokyo, Japan) to prepare recombinant plasmid for sensitivity test of the PCR. To monitor the sensitivity of the PCR, serial tenfold dilutions of the plasmid DNA (2×10^6 copies to 2 copies) were prepared using 1 μg/μl PCR test-negative genomic DNA from uninfected macaque peripheral blood mononuclear cells (PBMCs). The PCR reaction was performed in duplicate for each dilution, with inclusion of negative, positive, and reagent controls. The nested PCR reaction also was performed in duplicate, by using 2 μl of the first-round PCR reaction as described.

DNA sequencing and analysis. PCR products were purified using an Ultra Clean GelSpin Kit (MO BIO Laboratories, Inc., Solana Beach, Calif.) and directly sequenced using the BigDye Terminator v1.1 Cycle Sequencing Kit (Applied Biosystems, Tokyo, Japan) according to the manufacturer's protocol. The cycle sequencing reactions was performed as follows: initial denaturation at 96°C for 1 min; 25 cycles at 96°C for 10 sec, 50°C for 5 sec, and 60°C for 4 min. Electrophoresis of the samples was performed on an ABI PRISM 3100-Avant Genetic Analyzer (Applied Biosystems), and sequence analyses performed with GENETYX version 10.1.4 (Genetyx, Tokyo, Japan).

Results

SRV/D-T-specific PCR and sensitivity of PCR. SRV/D-T-specific primers were designed based on the nucleic acid sequences in the *gag* region of SRV/D -1, -2, and -3 and SRV/D-T (Table 1). First-round PCR using the SRV/D-T-specific primer set (Tga1 and Tga2) yielded a 722-bp product from genomic DNA of

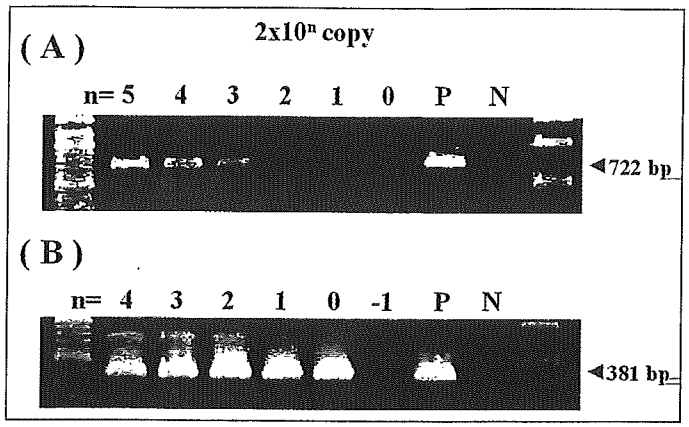

Figure 2. Sensitivity of PCR assays using SRV/D-T-specific primer sets. (A) Agarose gel electrophoresis of first-round PCR products on plasmid template with the Tga1 and Tga2 primers in the presence of 1 μg genomic DNA from macaque blood cells. (B) Agarose gel electrophoresis of nested PCR products with the Tga3 and Tga4 primers.

SRV/D-T infected Raji cells (Fig. 1A); no product was detected from monkey blood cell DNA samples. To increase the sensitivity and specificity, nested PCR was performed using a second primer set (Tga3 and Tga4) to amplify a 381-bp band (Fig. 1B). Products were not obtained from SRV/D-1 or -2 proviral DNA, showing the specificity of the Tga1 through Tga4 PCR primers for SRV/D-T. In contrast, in the first-round PCR, using the primer set for SRV/D subtypes 1 through 5 (SRVPOLF1 and SRVPOLR1) led to amplification of a 446-bp product from SRV/D-1, SRV/D-2, and SRV/D-T (Fig. 1C). In addition, the second round of nested PCR, using primers SRVPOLF2 and SRVPOLR2, led to amplification of a 181-bp fragment from SRV/D-1, SRV/D-2, and SRV/D-T as expected (Fig. 1D).

Using the cloned SRV/D-T *gag* plasmid, we determined the sensitivity of the PCR assay by end-point titration in the presence of carrier DNA. In first-round PCR using Tga1 and Tga2, as few as 2000 copies were detectable (Fig. 2A), whereas nested PCR adding Tga3 and Tga4 could detect as few as two genome copies (Fig. 2B).

Detection of SRV proviral DNA from macaque blood cells by SRV/D-T-specific PCR. SRV/D-T-specific PCR was performed using genomic DNA from whole peripheral blood cells of cynomolgus monkeys infected with SRV/D-T. As negative controls, DNA samples were prepared from blood of uninfected macaques. When genomic DNA from macaques infected with SRV/D-T was tested, the expected target 381-bp product was amplified effectively by nested PCR (Fig. 3A). However, using SRV/D-1 or -2 as template DNA for the nested PCR with these primers yielded no signal, and DNA from uninfected macaque blood lacked amplification of specific bands as well (Fig. 3A). Nested PCR using the SRVPOLF2 and SRVPOLR2 primers amplified a 181-bp fragment from blood-cell DNA from an SRV/D-T-infected macaque (Fig. 3B). Furthermore, the same 181-bp fragment was observed on macaque genomic DNA from uninfected monkeys (Fig. 3B). Because these generic primer sets from the *pol* region of SRV/D might also amplify endogenous type D retroviral sequences present in macaque genomic DNA (22) (Fig. 3B), we tested another primer set, which detects *gag* sequences of multiple SRV/D subtypes (Table 1, Fig. 3C). These results confirmed the specificity of the Tga primer sets for SRV/D-T and demonstrated

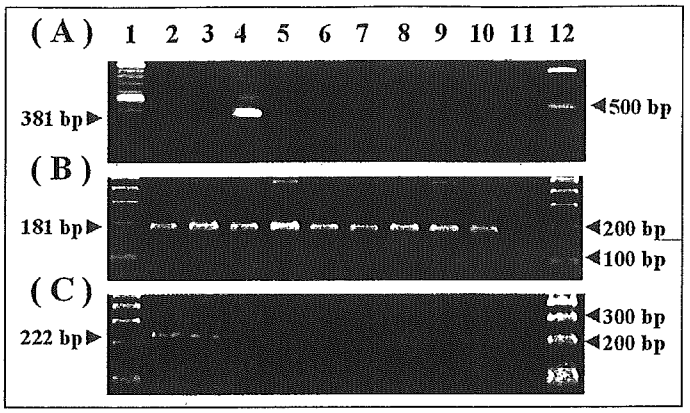

Figure 3. Detection of SRV/D-T signal from blood genomic DNA by nested PCR assay. (A) Tga1–Tga2 and Tga3–Tga4 primer sets were used for nested PCR amplification from blood genomic DNA of the monkey infected with SRV/D-T. (B) SRVPOLF1–SRVPOLR1 and SRVPOLF2–SRVPOLR2 primer sets. (C) WH1–WH3 and RC12–RC15 primer sets. Sources of template DNAs used are as follows: lane 2, Raji cells infected with SRV/D-1; lane 3, Raji cells infected with SRV/D-2; lane 4, blood cells from the monkey infected with SRV/D-T; lanes 5 through 10, blood cells from uninfected monkeys; lane 11, no DNA control. Lane 1, 100-bp ladder; lane 12, 1-kb or 100-bp ladder.

the lack of amplification of any endogenous SRV/D sequences by using these primer sets.

Survey of SRV/D infection in cynomolgus macaques at TPC. Previously, we reported the isolation of SRV/D-T from two cynomolgus monkeys in our breeding colony. However, it was unknown whether this subtype was prevalent in the TPC colony or if it were only a rare occurrence. To this end, EDTA-treated blood samples from 60 animals in the SPF colony and 49 retired breeders from the conventional colony were collected for genomic DNA preparation. We used the SRV/D-T-specific primer set and several other primer sets that detect other SRV/D subtypes (WH1-WH3 and RC12-RC13 for SRV/D-1 and -3 and WH1-WH3 and RC14-RC15 for SRV/D-2) (Table 1). Because the generic SRVPOLF2 and SRVPOLR2 primers appear to recognize endogenous SRV/D-related sequences (Fig. 3B), we did not use this primer set for direct detection of SRV/D from macaque blood DNA.

Using primers specific for SRV/D-1 and -3 or SRV/D-2, we detected no PCR signals for SRV/D in SPF or conventional monkeys. Use of the SRV/D-T specific primers also failed to amplify any products from the 60 SPF animals, confirming the SRV/D-free status of this colony. In contrast, SRV/D-T-specific primers amplified products from blood DNA samples from 11 of 49 monkeys (22.5%) from the conventional colony (Table 2). These 381-bp products were subjected to sequence analysis, and the results confirmed that all matched with that of SRV/D-T (data not shown). These results indicate that SRV/D subtypes 1 through 3 are not present in the TPC colony and that SRV/D-T is probably the only subtype. Regarding the SRV/D serology of the PCR-positive monkeys, three were seropositive, two were Western blot-indeterminate, and six were seronegative (10).

Discussion

The exogenous simian type D retroviruses occur in wild monkeys, are prevalent in captive populations of Asian macaque monkeys, and can cause immunodeficiency with anemia, weight loss, and persistent unresponsive diarrhea (2, 3, 5, 12). If macaques

Table 2. PCR-based survey of SRV/D infection in specific pathogen-free and conventional colonies at Tsukuba Primate Center

	Positive for			
	SRV/D-T	SRV/D-1, -2, -3	Negative	Total tests
SPF	0	0	60	60
Conventional	11	0	38	49

The blood DNAs from 60 cynomolgus monkeys in the SPF breeding colony and 49 animals in the conventional breeding colony were prepared as described in the Materials and Methods. The Tga1–Tga2 and Tga3–Tga4 primer sets were used to detect SRV/D-T sequences, WH1–WH3 and RC12–RC13 primer sets were used for SRV/D-1 and -3, and WH1–WH3 and RC14–RC15 primer sets used for SRV/D-2 (8).

infected with SRV/D are used in biomedical experiments, the results may be affected by the animal conditions and especially by the onset of clinical signs of disease including immunodeficiency (9). For these reasons, it is important to eliminate SRV/D infections from captive breeding colonies.

Since we established our indoor, closed cynomolgus monkey breeding colony, we have conducted periodical health examinations of all monkeys, including serum biochemistry and microbiological testing, every 2 years. Preliminary monitoring of SRV/D infection in our cynomolgus breeding colony indicated that approximately 20% of the animals were seropositive. We recently isolated a novel SRV/D subtype from two seropositive cynomolgus macaques in our conventional breeding colony that exhibited clinical signs of SRV/D infection. The *gag* region sequence of SRV/D-T differed from known SRV/D subtypes -1, -2, -3, and -5. Because some monkeys are inapparent virus carriers without detectable antibody responses (7), it is necessary to perform both serological testing and detection of virus presence in order to eradicate this virus from a breeding colony. To detect SRV/D-T specifically, we designed SRV/D-T-specific PCR primer sets based on the aligned gag sequences of SRV/D -1, -2, and -3 and SRV/D-T (Table 1). Using these specific primer sets, we were able to detect SRV/D-T-specific 722-bp and 381-bp products in first-round and nested PCR assays, respectively (Fig. 1). Moreover, the nested PCR for SRV/D-T was sensitive enough to detect as few as two copies of the viral genome (Fig. 2B). In order to simplify the testing procedure, we introduced the method of preparing genomic DNA directly from whole blood treated with EDTA. Using such genomic DNA as template for nested PCR, we were able to detect SRV/D-T directly in DNA prepared from blood cells of infected monkeys without having to purify PBMCs (Fig. 3A).

Although we isolated SRV/D-T from two cynomolgus monkeys in our breeding colony, it was unknown whether this subtype is prevalent at TPC. In order to investigate the subtypes of SRV/D present in our cynomolgus monkey colony, we used our SRV/D-T-specific primer sets and published primers that detect other SRV/D subtypes (8). Genomic DNA samples from the conventional and SPF monkey colonies were surveyed. The PCR-positive rate for SRV/D infection in retired breeders from the conventional colony was 22.4% (11 of 49), whereas no positive monkeys were detected in the SPF colony. Primer sets that simultaneously detect multiple SRV/D subtypes failed to identify SRV/D signals in either colony. Furthermore, 12 SRV/D isolates from captive-bred cynomolgus macaques housed in two separate buildings at TPC also were demonstrated to be SRV/D-T by sequence analysis of PCR products (data not shown). Therefore, we conclude that SRV/D-T is the major subtype of SRV/D present in the TPC conventional breeding colony.

There are several possibilities for the dominance of subtype SRV/D-T in the TPC colony. First, when the monkeys were imported from Southeast Asian countries, perhaps most were not infected with SRV/D, and only a few were infected with subtype SRV/D-T. This scenario seems unlikely because of a report of the isolation of SRV/D-2 from Indonesian cynomolgus monkeys (16). Therefore, we expect that the Indonesian cynomolgus monkeys in our breeding colony would have been infected with both SRV/D-2 and SRV/D-T. A second possibility is that particular subtypes of SRV/D endemic to monkeys in each country were introduced into the colony through importation. If this were the case, we have to consider why only SRV/D-T survived in the colony. Although further virological studies on SRV/D isolates are needed, SRV/D-T may have unique biological characteristics—such as abundant shedding of the virus in body fluids, increased stability of shed virus, higher infectivity, and/or increased replication rate—that allowed it to be readily transmitted within the colony from only a few infected monkeys. Considering the morphology, titer in cell culture, and genome structure of SRV/D-T, this possibility seems unlikely.

As previously described, to establish a large cynomolgus monkey breeding colony, we imported monkeys from the Philippines, Indonesia, and Malaysia between 1979 and 1983. After establishment of a closed breeding colony, periodic health examination with serum banking was conducted every year, and mating records, pedigrees, and daily observation records were all archived. Screening of banked sera dating from the original quarantine period may help identify the origin of SRV/D-T. Alternatively, it may be necessary to screen wild monkeys from each country of Southeast Asia by using our established PCR method to detect SRV/D-T and determine its origin.

Acknowledgments

We thank the animal caretakers at the Corporation for Production and Research of Laboratory Primates for giving us daily information on the monkey health conditions. We also thank R. Eberle (Department of Veterinary Pathobiology Oklahoma State University College of Veterinary Medicine) for critical reading of the manuscript. This work was supported in part by a grant from the Ministry of Health, Labor, and Welfare of Japan.

References

1. **Ageyama, N., Y. Hanazono, H. Shibata, K. Ohto, F. Ono, T. Nagashima, Y. Ueda, R. E. Donahue, M. Hasegawa, K. Ozawa, Y. Yoshikawa, and K. Terao.** 2002. Safe and efficient methods of autologous hematopoietic stem cell transplantation for biomedical research in cynomolgus monkeys. Comp. Med. **52:**445-451.
2. **Daniel, M. D., N. W. King, N. L. Letvin, R. D. Hunt, P. K. Sehgal, and R. C. Desrosiers.** 1984. A new type D retrovirus isolated from macaques with an immunodeficiency syndrome. Science **223:**602-605.
3. **Gardner, M. B., P. Luciw, N. Lerche, and P. Marx.** 1988. Nonhuman primate retrovirus isolates and AIDS. Adv. Vet. Sci. Comp. Med. **32:**171-226.
4. **Hara, M., T. Sata, T. Kikuchi, N. Nakajima, A. Uda, K. Fujimoto, T. Baba, and R. Mukai.** 2005. Isolation and characterization of a new SRV/D subtype from monkeys at Tsukuba Primate Center, Japan. Microbes Infect. **7:**126-131.
5. **Henrickson, R. V., D. H. Maul, K. G. Osborn, J. L. Sever, D. L. Madden, L. R. Ellingsworth, J. H. Anderson, L. J. Lowenstine, and M. B. Gardner.** 1983. Epidemic of acquired immunodeficiency in rhesus monkeys. Lancet **1:**388-390.
6. **Honjo, S.** 1985. The Japanese Tsukuba Primate Center for Medical Science (TPC): an outline. J. Med. Primatol. **14:**75-89.
7. **Kwang, H. S., N. C. Pedersen, N. W. Lerche, K. G. Osborn, P. A. Marx, and M. B. Gardner.** 1987. Viremia, antigenemia, and serum antibodies in rhesus macaques infected with simian retrovirus type 1 and their relationship to disease course. Lab. Invest. **56:**591-597.
8. **Lerche, N. W., R. F. Cotterman, M. D. Dobson, J. L. Yee, A. N. Rosenthal, and W. M. Heneine.** 1997. Screening for simian type-D retrovirus infection in macaques, using nested polymerase chain reaction. Lab. Anim. Sci. **47:**263-268.
9. **Lerche, N. W. and K. G. Osborn.** 2003. Simian retrovirus infections: potential confounding variables in primate toxicology studies. Toxicol. Pathol. **31(Suppl.):**103-110.
10. **Lerche, N. W., W. M. Switzer, J. L. Yee, V. Shanmugam, A. N. Rosenthal, L. E. Chapman, T. M. Folks, and W. Heneine.** 2001. Evidence of infection with simian type D retrovirus in persons occupationally exposed to nonhuman primates. J. Virol. **75:**1783-1789.
11. **Li, B., M. K. Axthelm, and C. A. Machida.** 2000. Simian retrovirus serogroup 5: partial gag-prt sequence and viral RNA distribution in an infected rhesus macaque. Virus Genes **21:**241-248.
12. **Marx, P. A., D. H. Maul, K. G. Osborn, N. W. Lerche, P. Moody, L. J. Lowenstine, R. V. Henrickson, L. O. Arthur, R. V. Gilden, and M. Gravell.** 1984. Simian AIDS: isolation of a type D retrovirus and transmission of the disease. Science **223:**1083-1086.
13. **Matano, T., M. Kano, T. Odawara, H. Nakamura, A. Takeda, K. Mori, T. Sato, and Y. Nagai.** 2000. Induction of protective immunity against pathogenic simian immunodeficiency virus by a foreign receptor-dependent replication of an engineered avirulent virus. Vaccine **18:**3310-3318.
14. **Mukai, R., T. Narita, R. Kobayashi, M. Fujimoto, M. Takasaka, and S. Honjyo.** 1992. Survey of viral infections in nonhuman primates at Tsukuba Primate Center for Medical Science, p. 399-408. *In* T. Nishida (ed.), Topics in primatology, vol. 3. University of Tokyo Press, Tokyo.
15. **Nandi, J. S., V. Bhavalkar-Potdar, S. Tikute, and C. G. Raut.** 2000. A novel type D simian retrovirus naturally infecting the Indian Hanuman langur (*Semnopithecus entellus*). Virology **277:**6-13.
16. **Pamungkas, J., J. T. Bieliitzki, R. A. Watanabe, M. Thouless, L. Kuller, A. M. Schmidt, C.-C. Tsai, D. Sajuyhi, and W. R. Morton.** 1992. Presence of certain infectious diseases in feral *M. facicularis* from Indonesia, p. 303-305. *In* American Association of Zoo Veterinarians (AAZV) Annual Proceedings. AAZV, Lawrence, Kans.
17. **Power, M. D., P. A. Marx, M. L. Bryant, M. B. Gardner, P. J. Barr, and P. A. Luciw.** 1986. Nucleotide sequence of SRV-1, a type D simian acquired immune deficiency syndrome retrovirus. Science **231:**1567-1572.
18. **Primate Society of Japan.** 1986. Guiding principles of animal experiments using nonhuman primates. Primate Res. **2:**111-113.
19. **Sonigo, P., C. Barker, E. Hunter, and S. Wain-Hobson.** 1986. Nucleotide sequence of Mason-Pfizer monkey virus: an immunosuppressive D-type retrovirus. Cell **45:**375-385.
20. **Takano, J., T. Narita, K. Fujimoto, R. Mukai, and A. Yamada.** 2001. Detection of B virus infection in cynomolgus monkeys by ELISA using simian agent 8 as alternative antigen. Exp. Anim. **50:**345-347.
21. **Thayer, R. M., M. D. Power, M. L. Bryant, M. B. Gardner, P. J. Barr, and P. A. Luciw.** 1987. Sequence relationships of type D retroviruses which cause simian acquired immunodeficiency syndrome. Virology **157:**317-329.
22. **van der Kuyl, A. C., R. Mang, J. T. Dekker, and J. Goudsmit.** 1997. Complete nucleotide sequence of simian endogenous type D retrovirus with intact genome organization: evidence for ancestry to simian retrovirus and baboon endogenous virus. J. Virol. **71:**3666-3676.
23. **Wang, Y. and M. E. Thouless.** 1996. Use of polymerase chain reaction for diagnosis of type D simian retrovirus infection in macaque blood. Lab. Anim. Sci. **46:**187-192.

Parasitol Res (2005) 97: 255–257
DOI 10.1007/s00436-005-1415-6

SHORT COMMUNICATION

**Jun-ichiro Takano · Toyoko Narita · Hiroshi Tachibana
Toshiyuki Shimizu · Hirofumi Komatsubara · Keiji Terao
Koji Fujimoto**

Entamoeba histolytica and *Entamoeba dispar* infections in cynomolgus monkeys imported into Japan for research

Received: 13 May 2005 / Accepted: 18 May 2005 / Published online: 1 July 2005

Abstract Three hundred and three stool samples of cynomolgus monkeys (*Macaca fascicularis*) imported from China and the Philippines were examined for *Entamoeba histolytica*/*Entamoeba dispar* infections. Microscopy detected *E. histolytica*/*E. dispar* cysts in 41 samples. Positive rates were higher in the monkeys from China (37.5%) than in the monkeys from the Philippines (3.7%). PCR analysis of 25 samples successfully cultured from the cysts demonstrated that 24 were *E. dispar*, one of the samples from China was *E. histolytica*. The one sample was also identified as *E. histolytica* by an antigen detection kit, although the monkey was asymptomatic and serology was negative. To our knowledge, this is the first report of *E. histolytica* isolation from cynomolgus monkeys based on the discrimination between *E. histolytica* and *E. dispar*.

Introduction

Amoebiasis, caused by infection with *Entamoeba histolytica*, is one of the most important parasitic diseases of humans. In addition to symptomatic cases such as hemorrhagic colitis and liver abscesses, asymptomatic infections, in which only cysts are passed in the feces, also exist. Therefore, discrimination between *E. histolytica* and the morphologically indistinguishable but non-pathogenic *E. dispar* is requisite (WHO 1997).

Amoebiasis has also been reported in captive and in wild-trapped non-human primates (Amyx et al. 1978; Beaver et al. 1988). However, recent studies have demonstrated the prevalence of *E. dispar* infections, but not *E. histolytica*, in 17 species of captive non-human primates (Smith and Meerovitch 1985), baboons (Jackson et al. 1990), Japanese macaques (Rivera and Kanbara 1999), seven species of captive Old World *Macaca* monkeys (Tachibana et al. 2001) and chimpanzees (Tachibana et al. 2000). In Japan, cynomolgus monkeys (*Macaca fascicularis*) have been imported for experimental use in medical research. However, the prevalence of *E. histolytica*/*E. dispar* infections, based on discrimination between the two species, is unknown. In the present study, we surveyed imported monkeys for *E. histolytica* and *E. dispar* infections.

Materials and methods

Stool samples were obtained from 215 cynomolgus monkeys from the Philippines by five different shipments and from 88 cynomolgus monkeys from China by four different shipments from 2000 April to 2002 June. Microscopic observation of trichrome-stained stool smears was performed to detect *E. histolytica*/*E. dispar* cysts. Stools with cysts were cultured xenically in Robinson's medium (Robinson 1968). After 3 days of cultivation, trophozoites were collected by centrifugation using a Percoll-gradient, as described by Tachibana et al. (1990). Genomic DNA of the trophozoites was extracted by a single-tube PCR kit (Takara) and then subjected to PCR amplification using primer sets specific for *E. histolytica* (p11 plus p12) and for *E. dispar* (p13 plus p14), as described by Tachibana et al. (1991). An antigen-capture

J. Takano (✉) · T. Narita · K. Fujimoto
The Corporation for Production and Research of Laboratory Primates, 1 Hachimandai, Tsukuba-shi Ibaraki, 305-0843, Japan
E-mail: takano@primate.or.jp
Tel.: +81-29-8372121
Fax: +81-29-8372299

H. Tachibana
Department of Infectious Diseases, Tokai University School of Medicine Bohseidai, Isehara-shi Kanagawa, 259-1193, Japan

T. Shimizu · H. Komatsubara
HAMRI Co., Ltd, 2638-2 Ozaki, Sanwa-machi, Sashima-gun Ibaraki, 306-0101, Japan

K. Terao
Tsukuba Primate Research Center, National Institute of Biomedical Innovation, 1 Hachimandai, Tsukuba-shi Ibaraki, 305-0843, Japan

ELISA for *E. histolytica* was performed with the *E. histolytica* II kit (TechLab), using cultured trophozoites. Serodiagnosis for *E. histolytica*-infection was performed by an indirect immunofluorescent test, using Amoeba-Spot IF (bioMerieux).

Results

The results of the microscopic and PCR tests are summarized in Table 1. *E. histolytica/E. dispar* cysts were detected in 13.5% (41/303) of the stools. The positive rates varied among the different shipments and countries from 2.3 to 66.7%. The cyst-positive rate in the shipments from China, 37.5%, was much higher than that from the Philippines, 3.7%. When the 41 cyst positive samples were cultured in Robinson's medium, 25 samples were grown successfully. The main cause of the failure of culture in 16 samples was an outgrowth of *Blastocystis hominis* trophozoites. PCR analysis of the 25 samples revealed that 24 were *E. dispar* and one was *E. histolytica*. No mixed infections were found.

The trophozoites judged as *E. histolytica* by PCR showed a positive OD value of 1.78 in antigen detection ELISA, whereas all the other trophozoites, judged as *E dispar*, had negative OD values of less than 0.05. In the serological tests, none of the monkeys was scored as positive to *E. histolytica*, including the monkey with the *E. histolytica*-infection. The *E. histolytica*-positive monkey was judged to be asymptomatic.

Discussion

Recently, in Japan, *E. dispar* infections, but not *E. histolytica*, were reported in 43% of *M. fuscata* (Rivera and Kanbara 1999); in 66% of captive *Macaca* monkeys (Tachibana et al. 2001); and in 56% of chimpanzees (Tachibana et al. 2000). The dominance of *E. dispar* infections observed in the present study accords with these previous reports. However, PCR analysis in this study was done from cultured parasites and not directly from fecal samples. Recently, it has been shown that culture in particular underestimates *E. histolytica* infection (Blessmann et al. 2002). Therefore, we cannot exclude the possibility that the prevalence of *E. histolytica* might be biased in this study. The difference of positive rates between China and the Philippines may depend on the hygienic managements of the monkey colonies or may reflect different positive rates in wild macaques.

In the present study, one isolate was identified as *E. histolytica* based on PCR analysis of the peroxiredoxin gene and antigenicity of the surface lectin (Haque et al. 2000). It might be essential to discriminate the isolate with a closely related parasite, such as *Entamoeba chattoni* or *Entamoeba moshkovskii*. Since the cysts in stool smears had four nuclei, infection with *E. chattoni* was ruled out. In addition, the possibility of *E. moshkovskii* could be ruled out because the PCR analysis did not amplify peroxiredoxin genes of the parasite (Tachibana et al. 1991; Cheng et al. 2004). To date, a limited number of *E. histolytica* isolates from non-human primates has been reported, that is, in one Japanese macaque (Tachibana et al. 1990) and in three species of old world and three species of new world monkeys (Verweij et al. 2003). To our knowledge, this is the first report of the isolation of *E. histolytica* from cynomolgus monkeys based on the discrimination between *E. histolytica* and *E. dispar*.

Although the monkey infected with *E. histolytica* was asymptomatic and did not have a positive serology to *E. histolytica*, asymptomatic cyst passers can become symptomatic under immunosuppressive conditions. Furthermore, the *E. histolytica* cysts in the stool of infected monkeys represent a zoonotic hazard to the caretakers. Tests to differentiate between *E. histolytica* and *E. dispar*, followed by successful treatment to exclude *E. histolytica* from the monkeys, are essential for the safe use of monkeys in experiments.

Table 1 Detection of *E. histolytica/E. dispar* cysts in feces of cynomolgus monkeys and differentiation of both species by PCR analysis of cultured trophozoites

Country	Shipment	Number of monkeys	Number of positives by microscopy (%)		Number of successful cultures	Number of PCR positives	
						E. histolytica	*E. dispar*
Philippines	1	39	2	(5.1)	1	0	1
	2	44	2	(4.5)	1	0	1
	3	44	2	(4.5)	2	0	2
	4	44	1	(2.3)	1	0	1
	5	44	1	(2.3)	1	0	1
Subtotal		215	8	(3.7)	6	0	6
China	1	6	4	(66.7)	3	0	3
	2	50	20	(40.0)	7	0	7
	3	7	2	(28.6)	2	1	1
	4	25	7	(28.0)	7	0	7
Subtotal		88	33	(37.5)	19	1	18
Total		303	41	(13.5)	25	1	24

Acknowledgments This work was supported by grants from the Ministry of Health, Labor and Welfare of Japan (to H. Tachibana and K. Terao).

References

Amyx HL, Asher DM, Nash TE, Gibbs CJ, Gajdusek DC (1978) Hepatic amebiasis in spider monkeys. Am J Trop Med Hyg 27:888–891

Beaver PC, Blanchard JL, Seibold HR (1988) Invasive amebiasis in naturally infected New World and Old World monkeys with and without clinical disease. Am J Trop Med Hyg 39:343–352

Blessmann J, Buss H, Nü PAT, Dinh BT, Ngo QTV, Van AL, Alla MDA, Jackson TFHG, Ravdin JI, Tannich E (2002) Real-Time PCR for detection and differentiation of *Entamoeba histolytica* and *Entamoeba dispar* in fecal samples. J Clin Microbiol 40:4413–4417

Cheng XJ, Yoshihara E, Takeuchi T, Tachibana H (2004) Molecular characterization of peroxiredoxin from *Entamoeba moshkovskii* and a comparison with *Entamoeba histolytica*. Mol Biochem Parasitol 138:195–203

Haque R, Mollah NU, Ali IKM, Alam K, Eubanks A, Lyerly D, Petri WA Jr (2000) Diagnosis of amebic liver abscess and intestinal infection with the TechLab *Entamoeba histolytica* II antigen detection and antibody tests. J Clin Microbiol 38:3235–3239

Jackson TF, Sargeaunt PG, Visser PS, Gathiram V, Suparsad S, Anderson CB (1990) *Entamoeba histolytica*: naturally occurring infections in baboons. Arch Invest Med (Mex) 21(Suppl 1):153–156

Rivera WL, Kanbara H (1999) Detection of *Entamoeba dispar* DNA in macaque feces by polymerase chain reaction. Parasitol Res 85:493–495

Robinson GL (1968) The laboratory diagnosis of human parasitic amoebae. Trans R Soc Trop Med Hyg 62:285–294

Smith JM, Meerovitch E (1985) Primates as a source of *Entamoeba histolytica*, their zymodeme status and zoonotic potential. J Parasitol 71:751–756

Tachibana H, Kobayashi S, Kato Y, Nagakura K, Kaneda Y, Takeuchi T (1990) Identification of a pathogenic isolate-specific 30,000-Mr antigen of *Entamoeba histolytica* by using a monoclonal antibody. Infect Immun 58:955–960

Tachibana H, Kobayashi S, Takekoshi M, Ihara S (1991) Distinguishing pathogenic isolates of *Entamoeba histolytica* by polymerase chain reaction. J Infect Dis 164:825–826

Tachibana H, Cheng XJ, Kobayashi S, Fujita Y, Udono T (2000) *Entamoeba dispar*, but not *E. histolytica*, detected in a colony of chimpanzees in Japan. Parasitol Res 86:537–541

Tachibana H, Cheng XJ, Kobayashi S, Matsubayashi N, Gotoh S, Matsubayashi K (2001) High prevalence of infection with *Entamoeba dispar*, but not *E. histolytica*, in captive macaques. Parasitol Res 87:14–17

Verweij JJ, Vermeer J, Brienen EAT, Blotkamp C, Laeijendecker D, Lieshout LV, Polderman AM (2003) *Entamoeba histolytica* infections in captive primates. Parasitol Res 90:100–103

WHO (1997) *Entamoeba* taxonomy. Bull WHO 75:291–292

The Natural History Journal of Chulalongkorn University, Supplement 1: 79-83, October 2005

Using Long-tailed Macaques (*Macaca fascicularis*) as a Model for Osteoporosis Study

TAKASHI YOSHIDA

Tsukuba Primate Research Center, National Institute of Biomedical Innovation, Hachimandai 1, Tsukuba, Ibaraki 305-0843, JAPAN

ABSTRACT.- **Ovariectomized female long-tailed macaques were used as a human model for osteoporosis. Each animal was measured for total body characteristics and lumbar vertebrae characteristics by dual energy X-ray absorptiometory, and measured for biochemical markers of bone resorption and formation. The measurements showed that bone mineral content for the total body and for the lumbar vertebrae, and bone mineral density of lumbar vertebrae were significantly decreased after the ovariectomy. Although no changes were detected in the serum concentrations of the biochemical markers of bone resorption, significant increases were detected in the serum concentrations of the makers of bone formation. The process of loss of bone mass after ovariectomy is analyzed.**

KEY WORDS: Long-tailed macaque, Osteoporosis, Ovariectomy, Bone formation marker, Bone resorption marker

INTRODUCTION

Nonhuman primates are widely used in bone research due to similarities in their reproductive functions and skeletal systems to humans (Yoshida, 1999), including reproductive endocrinology (menarche, regular menstruation and spontaneous menopause), increased bone turnover and bone loss in association with estrogen depletion, and skeletal micro architecture as revealed by histomorphometry. Osteoporosis is one of the most common diseases in the aged and constitutes a significant public health problem in the world. Ovarian hormone deficiency is considered the major risk factor for osteoporosis. Several animal species have been used in studies on loss of bone mass, including rat, mice, and primates. Long-tailed macaques maintained at Tsukuba Primate Research Center have been used in several analyses of bone mass, bone gain with growth and bone loss with aging. The objective of this study was to clarify the process of bone loss after ovariectomy in matured female long-tailed macaques as the animal model of post-menopausal osteoporosis.

* Corresponding author.
E-mail: yoshida@nibio.go.jp

MATERIALS AND METHODS

Laboratory-bred long-tailed macaques (*Macaca fascicularis*) were used in this study. Fourteen animals were divided into two groups; ovariectomized (OVX) (seven animals, 14.3±1.8 years old); and control (seven animals, 15.1±2.5 years old). All animals were kept in individual cages in an air-conditioned room in which the temperature was maintained at 25 ± 2 °C, the relative humidity at 60 ± 5 %, and with artificial lighting between 0500-

TABLE 1. Measurement items

Item		Abbreviation
Whole body	Body weight	BW
	Lean tissue mass	Lean
	Fat tissue mass	Fat
	(Fat tissue mass)/(Lean tissue mass+Fat tissue mass) x 100	%Fat
	Bone mineral content	BMC_{TB}
Lumbar vertebrae	Bone mineral content	BMC_L
	Bone area	$Area_L$
	Bone mineral density	BMD_L
Biochemical markers of bone turnover		
Formation marker	Intact osteocalcin (bone Gla-protein)	OC (BGP)
	Bone alkaline phosphatase	B-ALP
	Amino-terminal propeptide of type 1 procollagen	P1NP
	Carboxy-terminal propeptide of type 1 procollagen	P1CP
Resorption marker	Pyridine cross-linked carboxyterminal teleopeptide of type 1 collagen	1CTP
	Tartrate-resistant acid phosphatase	TrACP
	Pyridinoline	Pyr
	Deoxypyridinoline	D-Pyr

1900h daily. They were fed commercially prepared monkey food, apples and oranges. The breeding procedure and the rearing conditions were the same as previously described (Honjo, 1985). Previously described methods were used for the measurement of total body characteristics (Narita et al., 1994) and lumbar vertebrae characteristics (Hiyaoka et al., 1994) by dual energy X-ray absorptiometory (DXA, Lunar DPX-α).

Table 1 lists the parameters that were measured, including biochemical markers of bone metabolism. Serum samples were used for determination of biomarkers excepting pyridinolin and deoxypyridinolin. These two markers were determined using urinary samples and corrected using urinary creatinine concentration as a standard.

RESULTS

Measured values for the OVX group were compared with those for the control group. Although no change in body weight after ovariectomy was observed in the OVX group, a significant decrease in the bone mineral content of the total body was detected (Fig. 1). No changes were detected in the lumber vertebrae (areas L3-L5) in the OVX group. However, the bone mineral content slightly decreased and the bone mineral density significantly decreased (Fig. 2). In the OVX group 16 weeks or more after overiectomy, the serum concentrations of B-ALP were significantly higher than those in the control group (Fig. 3). Both the serum concentrations of other bone formation markers in the OVX group tend to show higher values than those in the control group. In contrast, bone resorption markers in serum and urine samples showed no significant difference in the concentration between in the OVX group and in the control group (Fig. 4).

DISCUSSION

Because of their many similarities to humans, long-tailed macaques are frequently used in research on bone diseases (Bowles et al., 1985. Miller et al., 1986). In humans, although the data do not always concur, probably because of the different subjects nationalities (assumed genetic differences) or analysis methods used, most studies show that linear growth of bones ceases at around the age of 20 years, but that the bones continue to mineralize until bone mass peaks in the third decade of life. In our study, female long-tailed macaques manifested similar changes. The menarche of female long-tailed macaques occurs at about 2.5 years old and menopause at about 22 years with an estimated lifespan of over 30 years (Yoshida, 1990). In our study the

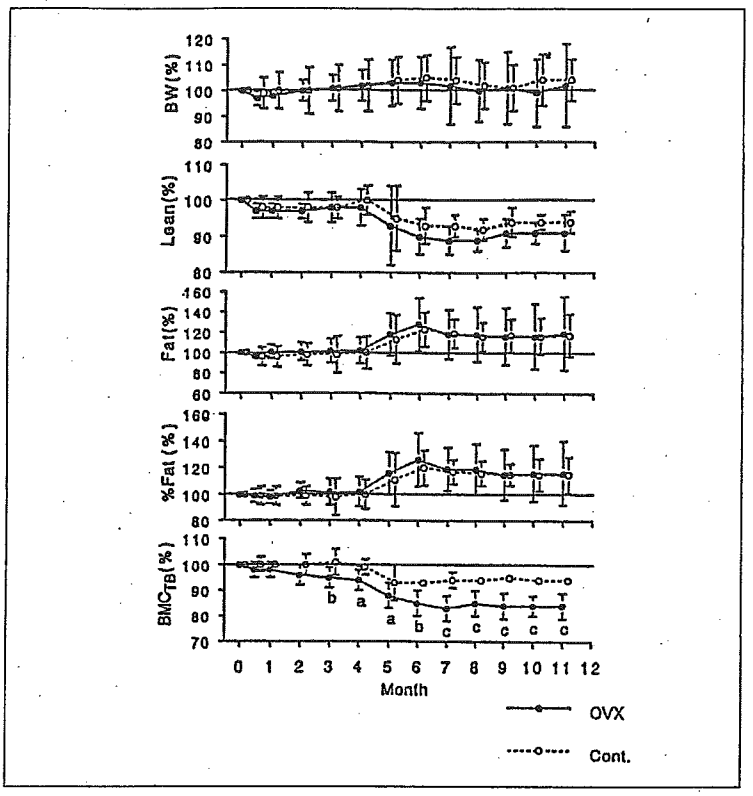

FIGURE 1. Measurements (Mean+SD) of whole body after ovariectomy in female cynomolgus monkeys (a; $p<0.05$, b; $p<0.01$, c; $p<0.001$).

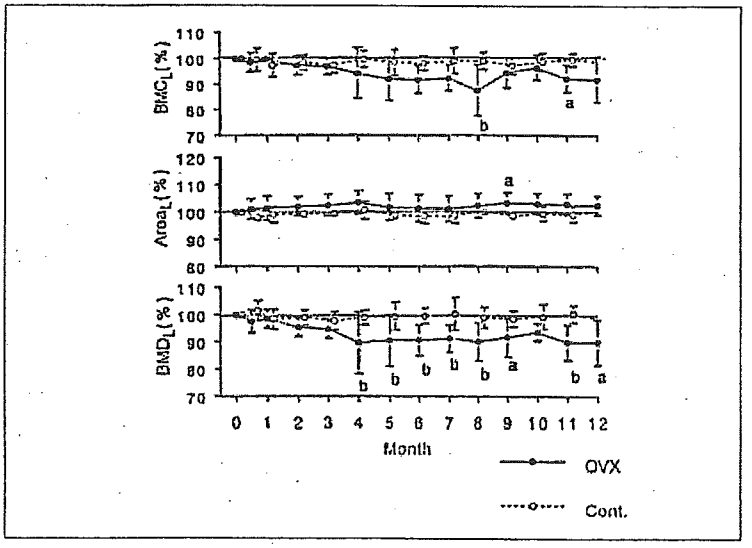

FIGURE 2. Measurements (Mean+SD) of lumbar vertebrae after ovariectomy in female cynomolgus monkeys (a; $p<0.05$, b; $p<0.01$).

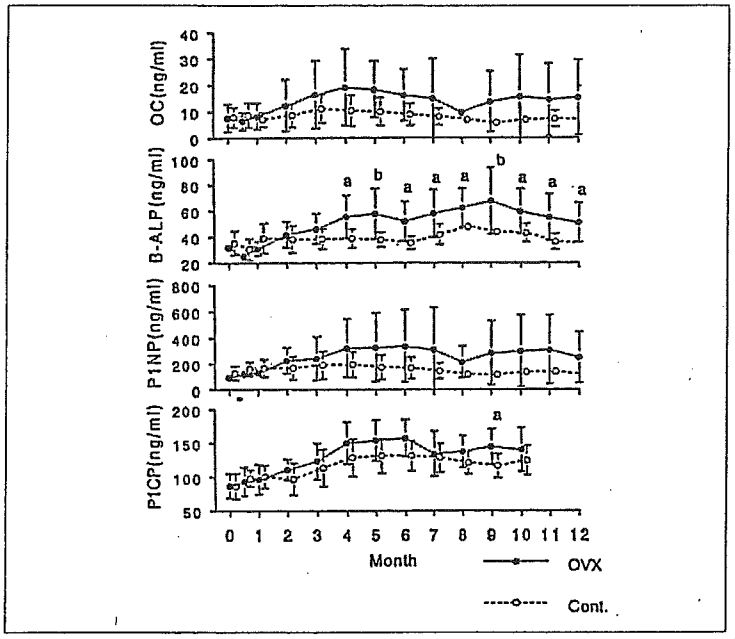

FIGURE 3. Measurements (Mean+SD) of serum bone formation markers after ovariectomy in female cynomolgus monkeys (a; $p<0.05$, b; $p<0.01$).

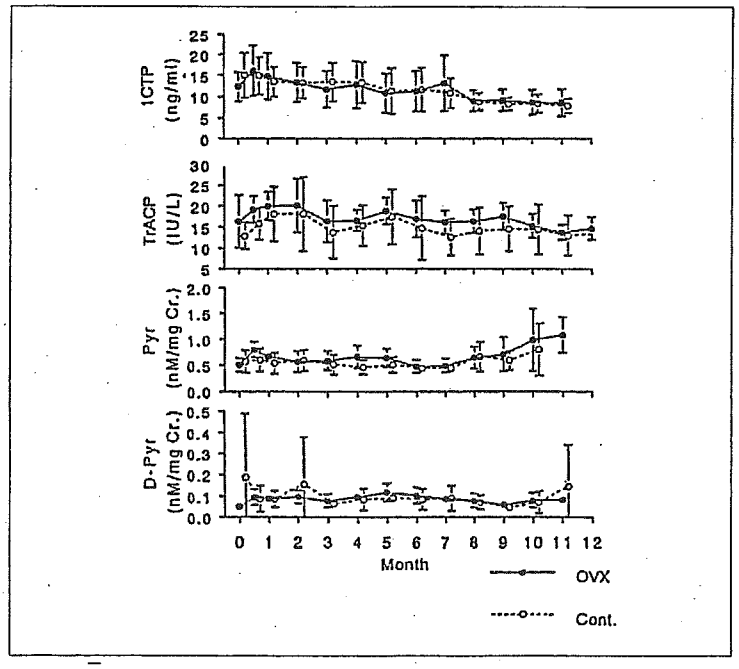

FIGURE 4. Measurements (Mean+SD) of serum urinary bone resorption markers after ovariectomy in female cynomolgus monkeys.

growth of the lumbar vertebrae was rapid during prepubecence, and then growth slowed after menarche. The bone mass peaked at about 9 years of age (Chen et al., 2000). Jayo et al. (1994) suggested that female long-tailed macaques achieve peak bone-mass at the age of 9, in agreement with our study, but they found that the bone mass tended to decrease in older mature animals of more than 13.5 years.

The significant reduction of the bone mineral content of the total body and the bone mineral density of the lumber vertebrae after ovariectomy were demonstrated. We suggest that the age of animals at ovariectomy is important to successfully induce the reduction of the bone mineral content and the bone mineral density after ovariectomy. Since we used animals over 9 years old in this study they had already achieved peak bone-mass.

Although serum concentrations of bone formation markers in the OVX group tend to show higher values than those in the control group, serum and urine concentrations of bone resorption markers showed no significant differences between two groups. This phenomenon may indicate accelerated bone formation with no change in bone resorption rates, but rather with a reduction in bone minerals. The reason for this discrepancy is not clear and further analyses are needed.

In conclusion, ovariectomized long-tailed macaques are judged to potentially be a suitable animal model for post-menopausal osteoporosis study.

LITERATURE CITED

Bowles, E. A., Weaver, D. S., Telewski, F. W., Wakefield, A. H., Jaffe, M. J. and Miller, L. C. 1985. Bone measurement by enhanced contrast image analysis: Ovariectomized and intact *Macaca fascicularis* as a model for human postmenopausal osteoporosis. American Journal of Physical Anthropology, 67: 99-103.

Chen, Y., Shimizu, M., Sato, K., Koto, M., Tsunemi, K., Yoshida, T. and Yoshikawa, Y. 2000. Effects of aging on bone mineral content and bone biomakers in female cynomologus monkeys. Experimental Animals, 49: 163-170.

Honjo, S. 1985. The Japanese Tsukuba Primate Center (TPC); An outline. Journal of Medical Primatology, 14: 75-89.

Hiyaoka, A., Yoshida, T., Cho, F. and Yoshikawa, Y. 1994. Age-related changes in bone mineral density, mean width and area of thee lumbar vertebrae in male African green monkeys (*Cercopithecus aethiops*). Experimental Animals, 43: 235-241.

Jayo, M. J., Jerome, C. P., Lee, C. J., Rankin, S. E. and Weaver, D. S. 1994. Bone mass in female cynomolgus macques: A cross-sectional and longitudinal study by age. Calcified Tissue Internation, 54: 231-236.

Miller, L. C., Weaver, D. S., McAlister, J. A. and Koritnik, D. R. 1986. Effects of ovariectomy on vertebral trabecuular bone in the cynomologus monkey (*Macaca fascicularis*). Calcified Tissue Internation, 38: 62-65.

Narita, H., Ohkubo, F., Yoshida, T., Cho, F. and Yoshikawa, Y. 1994. Measuring bone mineral content and soft tissue mass in the living cynomologus monkey. Experimental Animals, 43: 261-265.

Yoshida, T. 1990. Growth and development of the laboratory-bred cynomologus monkey (*Macaca fascicularis*). Journal of Growth, 29: 75-118.

Yoshida, T. 1999. Similarities and differences in reproductive endocrinology between non-human primates and humans. Congenital Anomalies, 39: 209-222.

Received: 15 Auguest 2005
Accepted: 26 September 2005

ELSEVIER

Bone 38 (2006) 265–272

BONE

www.elsevier.com/locate/bone

Regional distinctions in cortical bone mineral density measured by pQCT can predict alterations in material property at the tibial diaphysis of the Cynomolgus monkey

Kiichi Nonaka [a,b,c,*], Satoshi Fukuda [b], Kazuhiro Aoki [a], Takashi Yoshida [d], Keiichi Ohya [a]

[a] *Section of Pharmacology, Department of Hard Tissue Engineering, Division of Bio-Matrix, Graduate School, Tokyo Medical and Dental University, Japan*
[b] *International Space Radiation Laboratory, National Institute of Radiological Sciences, Japan*
[c] *Section of Health Science, ELK Corporation, Japan*
[d] *Tsukuba Primate Research Center, National Institute of Biomedical Innovation, Japan*

Received 17 December 2004; revised 14 July 2005; accepted 17 August 2005
Available online 5 October 2005

Abstract

We examined whether regional differences in cortical bone mineral density (Ct.BMD) measured by peripheral quantitative computed tomography is related to the heterogeneity of bone tissue and whether regional Ct.BMD is a better indicator of changes in bone material properties. Bilateral tibiae were obtained from 17 female adult Cynomolgus monkeys (*Macaca fascicularis*; mean age 16.8 years). After determining that Ct.BMD was similar between the right and left tibiae, the left tibiae were used for bone histomorphometry and the right for a three-point bending test. The Ct.BMD in the posterior quadrant was significantly higher than that in the anterior quadrant. In the bone histomorphometric analysis, all parameters (i.e., average osteonal area, average osteonal bone area, osteon population density, percent osteonal area [%On.Ar], percent osteonal bone area [%On.B.Ar], percent osteonal area of initial remodeling [%Il.On.Ar], percent osteonal area of secondary remodeling [%Sd.On.Ar], porosity, and percent osteoid area in the posterior region) were significantly lower than those in the anterior region. The results indicated that in the same cross-section, bone tissue structure was heterogeneous. Both total- and posterior-Ct.BMD were positively correlated with breaking stress and negatively correlated with toughness, whereas anterior-Ct.BMD was positively correlated with elastic modulus. Backward stepwise multiple regression analyses indicated that posterior-Ct.BMD and total-Ct.BMD were the best variables for predicting breaking stress and toughness, respectively, when age is taken into account. The %On.Ar, %On.B.Ar, and %Il.On.Ar in the posterior region were negatively correlated with elastic modulus. The %On.Ar, %On.B.Ar, and %Sd.On.Ar in the posterior region were positively correlated with toughness. These findings indicated that regional Ct.BMD measurement is useful to assess changes in the material properties of bone associated with the degree of mineralization. In particular, anterior-, posterior-, and total-Ct.BMD can be used separately to predict changes in the material properties of the tibial diaphysis.

Keywords: pQCT; Cortical bone; Mechanical testing; Mineralization; Cynomolgus monkey

Introduction

Knowledge of both geometric and material properties is necessary to assess whole-bone mechanical properties [1–5]. Peripheral quantitative computed tomography (pQCT), which is widely used for animal experiments and clinical diagnosis, can be used to analyze section modulus and cross-sectional moment of inertia as geometric properties under bending or torsional loading conditions [6–11]. It can also be used to analyze volumetric cortical bone mineral density (Ct.BMD; g/cm^3), which may in turn be used to predict the mechanical properties of bone material [12,13]. In contrast, the value of bone mineral density (BMD; g/cm^2) obtained by dual-energy X-ray absorptiometry, which is also extensively used clinically [14–16], is expressed as bone mineral content per projected bone area. Because the BMD determined by dual-energy X-ray absorptiometry derives from the sum of both trabecular and cortical bone mineral content and is dependent

* Corresponding author. Section of Health Science, ELK Corporation, 2-17-4, Yushima, Bunkyo-Ku, Tokyo 113-0034, Japan. Fax: +81 3 3818 9385.
E-mail address: kiichi_nonaka@elkc.co.jp (K. Nonaka).

8756-3282/$ - see front matter © 2005 Elsevier Inc. All rights reserved.
doi:10.1016/j.bone.2005.08.012

on bone size, it is not a predictor of the tissue material properties and is fundamentally different from Ct.BMD determined by pQCT.

Previous studies indicate that toughness of human bone is negatively correlated with age and ash content [17,18], that is, older bone is less tough than younger bone due to the high degree of mineralization. Decreased toughness reduces the ability of bone to absorb the energy of impacts and makes it more brittle. Although increased mineralization increases bone strength in static tests, it reduces toughness and makes bone more likely to fracture on impact. Although Ct.BMD positively relates to breaking stress and elastic modulus [12,13], the relationship between Ct.BMD and toughness remains unclear [19–21]. Ct.BMD is calculated from the whole cortical bone area based on the assumption of homogeneity. There is, however, some heterogeneity in bone tissue, such as porosity, remodeling, microdamage accumulation, osteonal population density, and mineralization [22–27].

We hypothesized that, in the same cross-section, there are regional differences in Ct.BMD measured by pQCT. Our objective was to examine whether regional analysis of Ct. BMD, measured by pQCT, could improve the assessment of material properties by analyzing its relation to the values of intracortical bone histomorphometry and structural mechanical testing in the tibial diaphysis of Cynomolgus monkey.

Materials and methods

Experimental animals

Seventeen female Cynomolgus monkeys (*Macaca fascicularis*), aged 16.8 ± 2.6 y (mean ± SD) and weighing 4.6 ± 1.1 kg, were used. All animals were bred in a cage with standard diets at the Tsukuba Primate Research Center, National Institute of Biomedical Innovation, and had no diseases that affect bone metabolism. After the animals were euthanized, all extremities were fixed in 10% neutral buffered formalin, and the soft tissue was removed. Thereafter, the tibiae were excised and transferred to 70% ethyl alcohol. The lengths of the right tibiae were measured using calipers (120.4 ± 5.1 mm). All animals in the study were treated and/or handled according to the "Recommendations for the Handling of Laboratory Animals for Biomedical Research" at Tsukuba Primate Research Center.

Bone densitometry

The mid-diaphyses of the right and left tibiae were scanned using a pQCT device (XCT Research SA+, Stratec Medizintechnik GmbH, Pforzheim, Germany) with pixel dimensions of 0.3 mm × 0.3 mm and a slice thickness of 0.77 mm. Total-Ct.BMD was analyzed for the whole cortical compartment, which was determined using a threshold value of 690 mg/cm^3, using pQCT software, Rev. 5.40. We also analyzed cross-sectional moment of inertia about the x axis (I_x) and section modulus about the x axis (Z_x), which was defined as I_x divided by half the depth of the cross-section. The cross-sectional images were divided into quadrants to analyze regional Ct.BMD in the anterior and posterior regions (Fig. 1). The coefficients of variation (%CV; standard deviation/mean) in our laboratory were 0.35% for Ct.BMD, 1.38% for I_x, and 2.26% for Z_x. These values were averaged %CVs determined from five repeated measurements of each of three tibiae, with sample repositioning before each measurement.

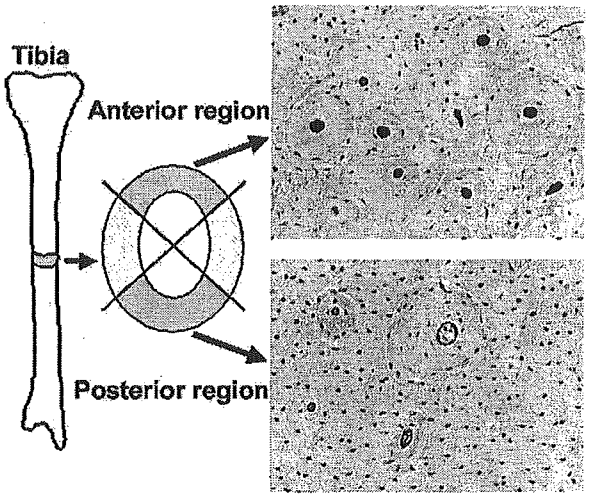

Fig. 1. Regions analyzed for pQCT and bone histomorphometry. Cross-sectional images measured by pQCT at the middle of the diaphyses were divided into quadrants. Cortical bone mineral density (Ct.BMD) was obtained from the total, anterior, and posterior cortex regions. The cross-sections of bone histomorphometry were also divided into quadrants to distinguish the anterior and posterior regions, corresponding to the same regions analyzed by pQCT.

Bone histomorphometry

Tissue preparation

Bone samples (7 mm thick) were taken from the middle of the left tibiae, immersed in Villanueva's bone stain solution, and later embedded in methylmethacrylate. Sections (25 μm thick) were prepared from the bone blocks using an auto-microtome (SP1600, Leica, Nussloch, Germany) and mounted on glass slides.

Intracortical histomorphometry

Segmented images of bone samples (1300 × 1030 pixels) were recorded using a digitizing system (Axiovision, Carl Zeiss, Germany) attached to a microscope (AxioPhoto, Carl Zeiss, Germany) at 50× magnification. The whole cross-sectional image was later reconstructed using image editing software (Adobe Photoshop Elements, Adobe Systems Inc., San Jose, CA). The entire cross-sectional image was divided into quadrants to distinguish the anterior and posterior regions, corresponding to the same area analyzed by pQCT (Fig. 1). Cortical area (Ct.Ar) of the anterior and posterior cortices was measured from the reconstructed image. Bone histomorphometry was performed using image analysis software (KS-400, Carl Zeiss, Germany) at 100× magnification. Primary and secondary parameters are presented in Table 1. The variables employed for this study were as follows; average osteonal area (av-On.Ar), average osteonal bone area (av-On.B.Ar), osteon population density (On.D), percent osteonal area (%On.Ar), percent osteonal bone area (%On.B.Ar), percent osteonal area of initial remodeling (%Il.On.Ar), percent osteonal area of secondary remodeling (%Sd.On.Ar), porosity (Po), and percent osteoid area (% O.Ar). The histomorphometric nomenclature used is that of the American Society for Bone and Mineral Research Committee [28].

Mechanical testing

The mechanical properties of the right tibia were measured by a three-point bending method using a mechanical testing machine (MZ-500S, Maruto Co. Ltd., Tokyo, Japan). The bending load was applied on the posterior surface of tibia at a speed of 10 mm/min until fracture, with the anterior surface of the tibia facing downwards on end supports separated by 60 mm. Breaking force, stiffness (slope of the linear portion of the load deformation curve), and work of fracture (area under the load deformation curve before fracture) were measured as whole-bone mechanical properties [29,30]. These values were normalized by cross-sectional moment of inertia and section modulus analyzed by pQCT to

Table 1
Intracortical histomorphometric parameters

Name of parameters	Abbreviations	Definitions or formulas	Units
Primary parameters			
*Average osteonal area	av-On.Ar	Mean value of each osteonal area	μm^2
Average Haversian canal area	av-H.Ar	Mean value of each Haversian canal area	μm^2
Cortical area	Ct.Ar	Area of cortical tissue including pores	mm^2
Osteon number	On.N	Number of osteons	#
Osteonal area	On.Ar	Total area of all osteons including Haversian canals	μm^2
Osteonal area of initial remodeling	Il.On.Ar	Total area of osteons of initial remodeling	μm^2
Osteonal area of secondary remodeling	Sd.On.Ar	Total area of osteons of secondary remodeling	μm^2
Haversian canal area	H.Ar	Total area of all Haversian canals	μm^2
Porous area	Po.Ar	Total area of all intracortical pores including Haversian canals	μm^2
Osteoid area	O.Ar	Total area of all osteoid	μm^2
Secondary parameters			
*Average osteonal bone area	av-On.B.Ar	av-On.Ar–av-H.Ar	μm^2
Cortical bone area	Ct.B.Ar	Ct.Ar–Po.Ar	mm^2
Osteonal bone area	On.B.Ar	On.Ar–H.Ar	μm^2
*Osteon population density	On.Dn	On.N/Ct.Ar	$\#/mm^2$
*Percent osteonal area	%On.Ar	On.Ar/Ct.Ar	%
*Percent osteonal bone area	%On.B.Ar	On.B.Ar/Ct.B.Ar	%
*Percent osteonal area of initial remodeling	%Il.On.Ar	Il.On.Ar/Ct.Ar	%
*Percent osteonal area of secondary remodeling	%Sd.On.Ar	Sd.On.Ar/Ct.Ar	%
*Porosity	Po	Po.Ar/Ct.Ar	%
*Percent osteoid area	%O.Ar	O.Ar/Ct.B.Ar	%

Primary and secondary parameters of bone histomorphometry are presented. Asterisks show the variables used in this study.

obtain material properties such as breaking stress, elastic modulus, and toughness, using the following formulae [31]:

$$\text{Breaking stress} = (\text{Breaking force}) \times L \times c/4 \times I_x = (\text{Breaking force}) \times L/4 \times Z_x$$

$$\text{Elastic modulus} = (\text{Stiffness}) \times L^3/48 \times I_x$$

$$\text{Toughness} = 3 \times (\text{Work of fracture}) \times c^2/L \times I_x = 3 \times (\text{Work of fracture}) \times I_x/L \times Z_x^2$$

where L is the span length, and c is half the depth of the cross-section.

Statistical analysis

Statistical differences were tested by two-tailed paired Student's t test. Linear regression analysis was performed to test the relationships among Ct.BMD, histomorphometric parameters, and material properties. Multiple linear regression models were developed using backward stepwise analyses to determine which Ct.BMD of the three different regions contributed to the mechanical properties of bone material by considering the effects of age, body weight, and bone length. The initial model included all Ct. BMDs of three different regions with age, body weight, and bone length. An independent variable was entered into the model at $F > 3.5$ and was removed at $F \leq 3.5$. A P value of less than 0.05 was considered statistically significant. All statistical analyses were performed using the statistical analysis software package, STATISTICA (StatSoft Inc., Tulsa, OK).

Results

Difference in Ct.BMD between the right and left tibiae

There were no significant differences in total-, anterior-, or posterior-Ct.BMD between the right and left tibiae (Table 2).

Regional differences in Ct.BMD and histomorphometric parameters between anterior and posterior regions

Posterior-Ct.BMD was significantly higher than anterior-Ct.BMD (Table 3). The bone histomorphometry analyses revealed that the values of av-On.Ar, av-On.B.Ar, On.D, % On.Ar, %On.B.Ar, %Il.On.Ar, %Sd.On.Ar, Po, and %O.Ar in the posterior region were significantly lower than those in the anterior region.

Relationships of whole-bone mechanical properties to age, body weight, and bone length and the values of pQCT and bone histomorphometry

The correlations of whole-bone mechanical properties with age, body weight, and bone length and the values of pQCT and bone histomorphometry are shown in Table 4. Only stiffness was positively correlated with body weight. The effects of age, body weight, and bone length on each Ct.BMD were different. Ct.BMD in the right tibiae was measured to examine its relationship with mechanical properties. Breaking force and stiffness were correlated with geometry, but not with Ct.BMD. With regard to bone histomorphometry, %On.Ar, %On.B.Ar, and %Il.On.Ar in the posterior region were negatively correlated with stiffness. The %Sd.On.Ar in the posterior region was positively correlated with work of fracture. In the anterior region, there were no significant correlations between the values of bone histomorphometry and whole-bone mechanical properties.

Table 2
Differences in cortical bone mineral density between the right and left tibial diaphyses

	Right ($n = 17$)	Left ($n = 17$)	P value
Total-Ct.BMD (mg/cm^3)	1264.6 ± 26.6	1262.6 ± 29.7	0.369 (n.s.)
Anterior-Ct.BMD (mg/cm^3)	1237.1 ± 22.3	1237.2 ± 31.5	0.981 (n.s.)
Posterior-Ct.BMD (mg/cm^3)	1303.2 ± 26.7	1298.1 ± 27.6	0.231 (n.s.)

Ct.BMD, cortical bone mineral density; n.s., no significant difference between the right and left tibiae (level of significance: $P < 0.05$). Data are expressed as mean ± SD.

Table 3
Regional differences in cortical bone mineral density and histomorphometric parameters between the anterior and posterior regions in the tibial diaphyses

	Anterior region (n = 17)	Posterior region (n = 17)	P value
Bone densitometry			
Right-Ct.BMD (mg/cm^3)	1237.1 ± 22.3	1303.2 ± 26.7	<0.0001
Left-Ct.BMD (mg/cm^3)	1237.2 ± 31.5	1298.1 ± 27.6	<0.0001
Bone histomorphometry in the left tibiae			
av-On.Ar (μm^2)	18,913.7 ± 6096.5	12,236.5 ± 5178.7	<0.0001
av-On.B.Ar (μm^2)	17,580.7 ± 5759.0	11,129.7 ± 4996.7	<0.0001
On.Dn (#/mm^2)	13.44 ± 2.70	8.25 ± 3.83	<0.0001
%On.Ar (%)	23.61 ± 8.37	9.48 ± 5.93	<0.0001
%On.B.Ar (%)	22.73 ± 8.29	8.84 ± 5.85	<0.0001
%Il.On.Ar (%)	14.34 ± 5.65	8.05 ± 5.43	<0.001
%Sd.On.Ar (%)	9.27 ± 3.86	1.44 ± 1.13	<0.0001
Po (%)	3.16 ± 1.93	1.95 ± 0.78	<0.005
%O.Ar (%)	0.19 ± 0.09	0.03 ± 0.03	<0.0001

Ct.BMD, cortical bone mineral density; av-On.Ar, average osteonal area; av-On.B.Ar, average osteonal bone area; On.Dn, osteon population density; %On.Ar, percent osteonal area; %On.B.Ar, percent osteonal bone area; %Il.On.Ar, percent osteonal area of initial remodeling; %Sd.On.Ar, percent osteonal area of secondary remodeling; Po, porosity; %O.Ar, percent osteoid area. Data are expressed as mean ± SD.

Relationships of material properties to age, body weight, and bone length and the values of pQCT and bone histomorphometry

The correlations of material properties with age, body weight, and bone length and the values of pQCT and bone histomorphometry are shown in Table 5. Only breaking stress was correlated with age. Both total- and posterior-Ct.BMD were positively correlated with breaking stress and negatively correlated with toughness, whereas anterior-Ct.BMD was positively correlated with elastic modulus. The coefficient of determination (r^2) of total-Ct.BMD for breaking stress (r^2 = 0.397) was slightly higher than that of posterior-Ct.BMD (r^2 = 0.335). The r^2 value of posterior-Ct.BMD for toughness (r^2 = 0.392) was greater than that of total-Ct.BMD (r^2 = 0.250). Anterior-Ct.BMD had the highest r^2 value (r^2 = 0.435) in the relation between Ct.BMDs and elastic modulus. The significant relationship between Ct.BMD and each material property in Table 5 is also graphed in Fig. 2. With regard to the values of bone histomorphometry, %On.Ar, %On.B.Ar, and %Il.On.Ar in the posterior region were negatively correlated with elastic modulus. The %On.Ar, %On.B.Ar, and %Sd.On.Ar in the posterior region were

Table 4
Correlation of whole-bone mechanical properties with age, body weight, bone length, cortical bone mineral density, and histomorphometric parameters in the tibial diaphyses

	Age (n = 17)	Body weight (n = 17)	Bone length (n = 17)	Breaking force (n = 16)	Stiffness (n = 16)	Work of fracture (n = 16)
Age, body weight, and bone length						
Age		0.204 (0.042)	−0.127 (0.016)	−0.233 (0.054)	0.132 (0.017)	−0.439 (0.193)
Body weight			0.401 (0.161)	0.467 (0.218)	0.561 (0.315)*	0.010 (<0.001)
Bone length				0.394 (0.155)	−0.138 (0.019)	0.125 (0.016)
Bone densitometry in the right tibiae						
Total-Ct.BMD	−0.220 (0.049)	0.346 (0.120)	0.237 (0.056)	0.428 (0.183)	0.365 (0.133)	−0.369 (0.136)
Anterior-Ct.BMD	−0.435 (0.189)	0.035 (0.001)	−0.100 (0.010)	0.160 (0.026)	0.395 (0.156)	−0.242 (0.059)
Posterior-Ct.BMD	0.058 (0.003)	0.373 (0.139)	0.221 (0.049)	0.415 (0.173)	0.377 (0.142)	−0.462 (0.213)
Z_x	0.093 (0.009)	0.363 (0.132)	0.065 (0.004)	0.808 (0.653)*	0.556 (0.309)*	0.265 (0.070)
Bone histomorphometry in the left tibiae						
Anterior region						
On.Dn	−0.050 (0.003)	0.352 (0.124)	0.317 (0.100)	0.224 (0.050)	−0.005 (<0.001)	0.246 (0.060)
%On.Ar	0.333 (0.111)	0.103 (0.011)	0.273 (0.074)	−0.179 (0.032)	−0.354 (0.125)	−0.191 (0.037)
%On.B.Ar	0.314 (0.098)	0.083 (0.007)	0.264 (0.070)	−0.162 (0.026)	−0.364 (0.133)	−0.181 (0.033)
%Il.On.Ar	0.302 (0.091)	0.101 (0.010)	0.372 (0.138)	−0.215 (0.046)	−0.383 (0.147)	−0.244 (0.059)
%Sd.On.Ar	0.280 (0.078)	0.077 (0.006)	0.047 (0.002)	−0.059 (0.004)	−0.184 (0.034)	−0.041 (0.002)
Po	0.337 (0.113)	−0.154 (0.024)	0.154 (0.024)	0.106 (0.011)	−0.194 (0.038)	0.008 (<0.001)
%O.Ar	−0.378 (0.143)	−0.369 (0.136)	0.121 (0.015)	−0.196 (0.038)	−0.327 (0.107)	−0.196 (0.039)
Posterior region						
On.Dn	0.155 (0.024)	0.172 (0.030)	0.011 (<0.001)	−0.236 (0.056)	−0.270 (0.073)	0.427 (0.182)
%On.Ar	0.091 (0.008)	−0.072 (0.005)	0.191 (0.037)	−0.279 (0.078)	−0.511 (0.262)*	0.339 (0.115)
%On.B.Ar	0.058 (0.003)	−0.099 (0.010)	0.184 (0.034)	−0.276 (0.076)	−0.519 (0.269)*	0.329 (0.108)
%Il.On.Ar	0.106 (0.011)	−0.091 (0.008)	0.176 (0.031)	−0.368 (0.135)	−0.514 (0.264)*	0.237 (0.056)
%Sd.On.Ar	−0.031 (0.001)	0.062 (0.004)	0.157 (0.025)	0.306 (0.093)	−0.199 (0.040)	0.624 (0.389)*
Po	0.480 (0.230)	−0.225 (0.051)	0.124 (0.015)	−0.187 (0.035)	−0.316 (0.100)	−0.195 (0.038)
%O.Ar	−0.262 (0.069)	−0.060 (0.004)	−0.200 (0.040)	−0.260 (0.068)	−0.025 (<0.001)	−0.195 (0.038)

Breaking force, stiffness, and work of fracture were measured in the right tibiae. The left tibiae were used to analyze the relationships between histomorphometric parameters and bone length. Ct.BMD, cortical bone mineral density; Z_x, section modulus about x axis; On.Dn, osteon population density; %On.Ar, percent osteonal area; %On.B.Ar, percent osteonal bone area; %Il.On.Ar, percent osteonal area of initial remodeling; %Sd.On.Ar, percent osteonal area of secondary remodeling; Po, porosity; %O.Ar, percent osteoid area. The data of mechanical tests from one sample were excluded because its stiffness was an outlier. Asterisk shows significant correlation (level of significance: $P < 0.05$). Parentheses: coefficient of determination (r^2).